RSC Advances

PAPER

View Article Online
View Journal | View Issue

Cite this: *RSC Adv.*, 2024, **14**, 10280

Stimulus triggered release of actives from composite microcapsules based on sporopollenin from *Lycopodium clavatum*†

Muriel Lecoeuche,[a] Josef Borovička,[a] Amro K. F. Dyab [bc] and Vesselin N. Paunov *[b]

Smart drug delivery systems (SDDSs) are a paradigm shift in drug delivery, particularly in microencapsulation technology where the drug is released in response to an internal and/or external stimulus. In this study, a smart microencapsulation platform was developed using three different types of stimuli triggered release of a model active (rhodamine 6G) from sporopollenin from *Lycopodium clavatum*. Triggers were based on pH-, thermal- and near infrared light-sensitive polymer composition. Carbopol nanogel and methylcellulose were used as responsive aqueous polymers for pH and thermally triggered release, respectively. Methylcellulose loaded with active and gold nanoparticles was used for photothermal triggered release. The formulations were encapsulated into the empty cores of sporopollenin microcapsules using the compressed tablet technique. The pH triggered release of the active was achieved above pH 7, which was mediated by the swelling of the carbopol nanogel that forced its way out of the elastic trilite scars of the sporopollenin. Results from measuring the active fluorescent intensity and its content over time confirmed the crucial role of carbopol in the pH triggered release. For the thermo-sensitive polymer methylcellulose, it was found that the release of the active from methylcellulose loaded sporopollenin was triggered upon heating the system reaching 90% whereas it levelled out at 40% for methylcellulose-free sporopollenin. The maximum amount of active was released at around 55 °C, where the sol–gel transition of the methylcellulose starts. Photothermally triggered release using near infrared (NIR) laser revealed that the amount of active released from sporopollenin loaded with both gold nanoparticles and methylcellulose was approximately four times higher than that from sporopollenin loaded with methylcellulose/active only, confirming the key role of gold nanoparticles in the release *via* photothermal heating of the polymer formulation.

Received 9th January 2024
Accepted 16th March 2024

DOI: 10.1039/d4ra00236a

rsc.li/rsc-advances

1. Introduction

Microencapsulation technologies offer protection for the active ingredient from potentially harsh environments, masking undesired tastes, alleviating drug side effects and potentially enhancing patient compliance.[1–3] This is based on wrapping the active ingredients (core materials) within a shell (encapsulant), that acts as a physical protection barrier. The crucial role of microencapsulation is to deliver the protected core materials in targeted and controlled manner to enhance the therapeutic efficacy of the actives and mitigates effects arising from their reduced biostability, poor water solubility, and low bioavailability. The triggered release of core materials at the desired time and site could be achieved *via* designing smart drug delivery systems (SDDSs) where the stimuli responsive shell materials can respond to an internal (endogenous) and/or external (exogenous) stimulus.[4–6] Internal stimuli include pH, glucose, enzymes, and oxidation–reduction,[7,8] while magnetic fields,[9,10] light,[11] temperature,[9] ultrasound[12] and mechanical action (pressure, friction)[13,14] are examples of external stimuli. For the development of smart microcapsules, two protocols have mainly been used to produce changes in the microcapsules shell to control their payload release: (i) embedding or grafting the stimuli-responsive materials on the shell or its pores, respectively; (ii) swelling/deswelling or destruction of the stimuli-responsive shell material.[9,13–18] We propose in the current work a different strategy where the stimuli-responsive materials (Carbopol Aqua SF-1 nanogel or Methylcellulose), loaded with rhodamine 6G as a model active, is encapsulated within robust natural micro-shells derived from plant pollens. This allowed us to explore the feasibility of this platform to non-destructively trigger the active release using (i) pH, (b) thermal

[a]*Department of Chemistry, University of Hull, Hull, HU6 7RX, UK*
[b]*Department of Chemistry, Nazarbayev University, Kabanbay Batyr Avenue 53, Astana 010000, Kazakhstan. E-mail: vesselin.paunov@nu.edu.kz; Tel: +7-7172-709514*
[c]*Chemistry Department, Colloids & Advanced Materials Group, Faculty of Science, Minia University, Minia 61519, Egypt*

† Electronic supplementary information (ESI) available. See DOI: https://doi.org/10.1039/d4ra00236a

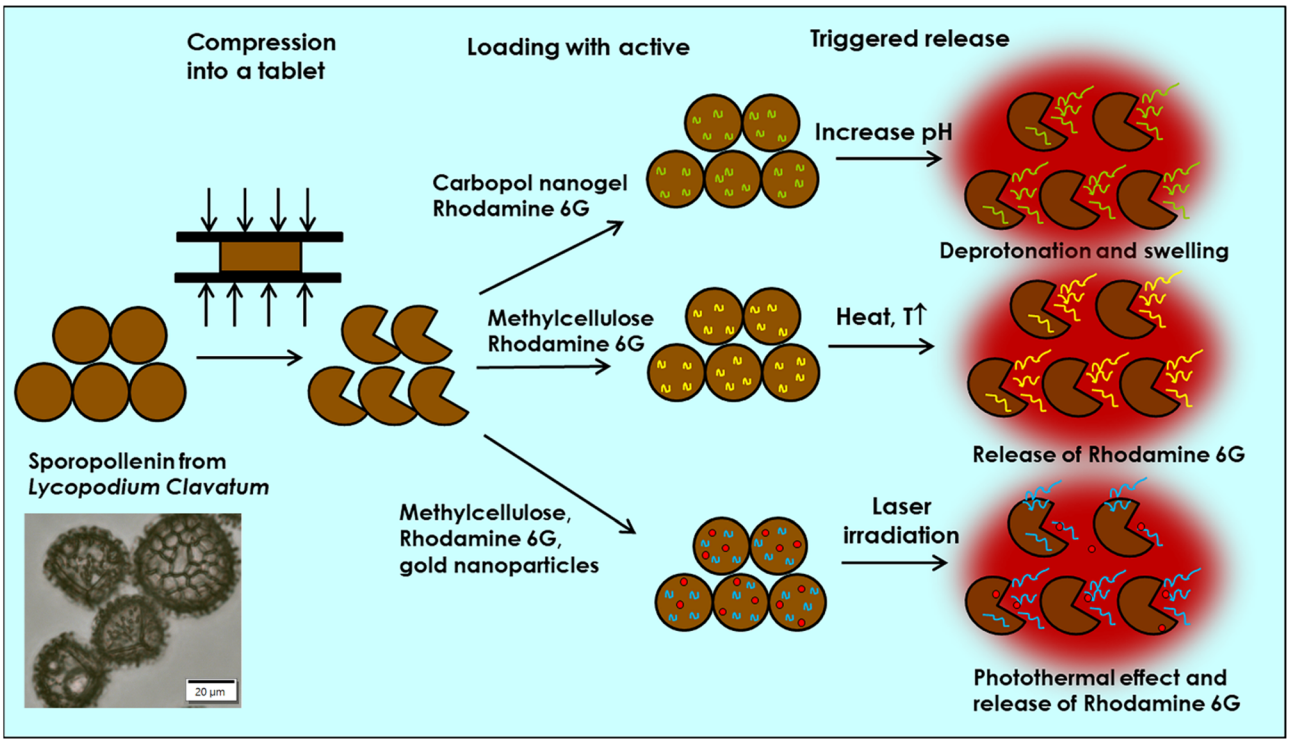

Fig. 1 Schematic representation of the preparation process of sporopollenin with Carbopol Aqua SF-1 nanogel loaded with a model active (rhodamine 6G). The acrylic co-polymer nanogel is pH sensitive and swells by increasing the pH above 7 thus allowing for pH triggered release. The nearly 10-fold increase of the nanogel volume inside the sporopollenin caused its ejection along with the encapsulated active which allows for pH-triggered payload release. Additionally, a heat triggered release was engineered by loading sporopollenin with methylcellulose solution along with the model active. Increasing of the temperature precipitates the methyl cellulose solution and releases the active out of the microcapsules. Light triggered release of active was also demonstrated by co-loading of the methylcellulose, the active and gold nanoparticles in sporopollenin.

and (iii) near infra-red (NIR) stimulus. The outer shell of plant pollens, obtained after removing the sporoplasm core, is called sporopollenin, which is considered to be one of the most resistant biopolymers found in nature.[19–21] Recently, sporopollenin has gained considerable attention as an effective encapsulation platform for several drugs[19,22–26] and biological substances.[27–30]

Compared to synthetic polymer-based drug microcarriers, sporopollenin microcapsules exhibit unique properties such as size uniformity, chemical and mechanical resistance, being cost-effective, nontoxic, allergy-free, providing UV protection and bio-adhesion.[20,24,26,31–33]

Nanogels are partially cross-linked hydrophilic or amphiphilic polymers that have the ability to encapsulate actives by hydrogen bonding, van der Waals forces, or electrostatic attraction.[34,35] Excessive attentions have been paid on stimuli-responsive nanogels to pH and/or temperature due to their significant potential in biomedical applications and drug release.[34,36,43–47] Carbopol Aqua SF-1 is a lightly cross-linked of acrylate copolymer which is commonly used as a rheology modifier in personal care products. This nanogel exhibits swelling ability, biocompatibility and low toxicity that entail its use in pH triggered drug delivery platforms where it swells in neutral and basic medium as a results of dissociation of its carboxyl groups (–COOH), promoting encapsulation of cationic actives.[31,35,37,38,43–47] Rhodamine 6G, a fluorescent dye of high photostability, was used here as a model active to be encapsulated into the Carbopol nanogel,[24] which allowed us to track its triggered release from sporopollenin microcapsules with various stimuli by using fluorescence microscopy.

Methylcellulose is a key material in pharmaceutical applications and is used to produce thermo-responsive and photothermal hydrogels.[39,40,42] At a critical temperature, these hydrogels undergo sol–gel transition, altering their physicochemical and mechanical properties, as well as their interaction with embedded actives. In addition, modified gold nanoparticles absorb near-IR light and released heat which can trigger the release of the active from the methylcellulose encapsulated into sporopollenin microcapsules. Fig. 1 shows the protocols used in the current study for exploring three types of stimulus-triggered release, where the combination of the unique properties of natural microcapsules and biocompatible materials may offer smart multifunction-controlled delivery platform for potential biomedical and drug delivery applications.

2 Experimental

2.1 Materials

Lycopodium clavatum pollen was supplied by Sigma-Aldrich, UK. Carbopol Aqua SF-1 (30 wt%) was obtained from Noveon, USA. Methylcellulose (Methocel A4M) was supplied by Dow, USA. Rhodamine 6G was supplied from Acros Organics, USA. Ethanol

(HPLC Grade), NaOH, HCl and NaCl (>98%) were purchased from Fisher Scientific, UK. All other reagents were of analytical grade and were used without further purification. Deionised (DI) water of resistivity of 18 MΩ cm^{-1} purified by reverse osmosis (Millipore®) was used in all experiments.

2.2 Methods

2.2.1 Swelling behavior of carbopol against pH. Carbopol Aqua SF-1 nanogel swelling behavior in aqueous solution was examined to evaluate its behavior with change of pH. For this purpose, a 1 wt% suspensions of carbopol were made from a 30 wt% stock suspension supplied by the manufacturer. Small aliquots of 0.1 M NaOH or 0.1 M HCl were then added to the samples to acquire solutions of a range of pH between 4 to 7.4 using pH meter (Fisherbrand Hydrus 300). Increasing the pH above 6 required the use of highly concentrated NaOH solutions. This observation can be explained by the ionization of the carboxylate groups around this pH. The particle hydrodynamic diameter was measured by Malvern Zetasizer with refractive index RI of 1.450 below pH 7 and for the swollen nanogel (above pH 7) with RI of 1.336. Two measurements were performed for the same pH. It is important to note that the samples were diluted to the right laser obscuration levels using DI water adjusted to the right pH using small aliquots of 0.1 M NaOH.

2.2.2 Encapsulation of rhodamine 6G-loaded carbopol nanogel into sporopollenin microcapsules. In order to obtain sporopollenin microcapsules devoid from the sporoplasm core we used the extraction protocol as described in previous work[27] and showed in ESI.† A 0.05 g tablet was first prepared from the sporopollenin powder (by using a tablet press with pressure of 10 tons). 10 mL of the Carbopol Aqua SF-1 nanogel was prepared by loading it with 1 mM rhodamine 6G dye followed by addition of 20 vol% ethanol. The sporopollenin tablet was then added to the nanogel suspension while stirring. Submitting the sporopollenin to high pressure allows squashing of its elastic capsules so that their trilite scars open to encapsulate the concentrated rhodamine 6G-loaded nanogel suspension. Ethanol improves the wetting of the sporopollenin interior to facilitate this loading process. The sample was then stirred for about 2 hours, dessicated and filtered by vacuum filtration set, and the solid was washed with 1 L of DI water. Washing the solid is an important step as it allows removal of the dye residue that has remained at the outer surface of the sporopollenin. A small amount of the washed sporopollenin was put into a Petri dish and suspended in DI water. The sample was observed under a fluorescence microscope BX-51 (Olympus, Japan) and CLSM to trace the location of the fluorescent dye and its release from the sporopollenin.

2.2.3 Quantitative characterization of the active release by measuring the fluorescence intensity. A sample of 0.477 mL of the aqueous suspension of the carbopol/rhodamine 6G loaded sporopollenin in DI water was then injected into a perfusion chamber (Grace BioLab coverwell, 622502, inner size 19 × 32 mm, inner depth 0.9 mm) placed on a glass microscope slide. To track the extent of release of the dye from the formulation, intensity recording was carried out to quantify the change in fluorescence intensity with time. The fluorescence intensity was measured using the software Image-Pro Plus with the profile line, on every image, the recording consisting in images taken with an interval of time of 300 ms. A line was placed on a precise spot of the image, and the data was exported which allowed providing the average intensity of every point of the line.

2.2.4 pH triggered release of rhodamine 6G. A 100 mL of rhodamine 6G-carbopol loaded sporopollenin suspension was split in two 200 mL beakers and both suspensions were agitated at the same time at 700 rpm and rhodamine 6G absorbance was measured at various times. Parafilm was placed on each beaker to prevent the dispersions from absorbing carbon dioxide and consequent acidification. At 10 min interval, eight drops of 0.1 M NaOH were added into one of the two beakers. The pH was measured at various times of the experiment. The amount of dye was calculated from the values of the concentration of the dye, which was determined using a UV-vis spectrophotometer (Varian Cary 50 Bio) using the calibration curve of rhodamine in DI water. The values of absorbance were measured at $\lambda = 525$ nm, which is the wavelength corresponding to the maximum absorbance of rhodamine in water. The trend after the addition of NaOH was the same for the three attempts, the amount of dye released suddenly rises and then continues increasing less sharply.

2.2.5 Thermally triggered release. To optimize the conditions for the thermos-responsive polymer for the encapsulation process, 1 wt% and 2 wt% dispersions of methylcellulose were prepared, by dissolving respectively 0.1 g and 0.2 g of Methocel A4M, respectively into 10 mL of DI water and stirring until complete dissolution. The size distribution of methyl cellulose dispersions was measured with the Mastersizer at both room temperature and after heating to 95 °C in a heating bath (grant, OLS 2000) for 30 min. The temperature of the solution inside the Mastersizer cell was recorded before starting the measurements. Encapsulation of rhodamine 6G-loaded methylcellulose into sporopollenin was performed as in Section 2.2.2. A sample of 0.477 mL of the aqueous suspension of the Methocel A4M/rhodamine 6G loaded sporopollenin in DI water was then injected into the perfusion chamber placed on a glass microscope slide. Scotch tape seals was placed onto the perfusion chamber openings, to prevent the evaporation of the aqueous phase during observations. The heating was performed by using a Peltier element mounted directly on the microscope stage starting from room temperature to 95 °C with a heating rate of 20 °C min^{-1}. Rhodamine 6G release from the sporopollenin was quantified by setting the temperature to 65 °C and measuring the change in fluorescence intensity with time using Image Pro Plus software.

A control experiment was recorded, by using the same heating parameters on a rhodamine 6G-loaded sporopollenin suspension without methylcellulose. The amount of rhodamine 6G released by the thermally triggering process was assessed by using 1 wt% methylcellulose and 1 mM of rhodamine 6G loaded into sporopollenin microcapsules. The loaded microcapsules were then washed with 3.5 L of DI water and suspended into 10 mL of DI water and placed into a heating bath with a shaking frequency of 144 min^{-1} at various temperatures for 20 min for each run. Two experiments were performed for each temperature. Eventually, the suspensions were filtered, and the absorbance of the filtrate was measured using UV-vis spectrophotometer.

2.2.6 Release of rhodamine 6G with NIR trigger. Four types of loaded sporopollenin samples were prepared to be irradiated with a NIR laser: (i) sporopollenin loaded with methylcellulose, 0.1 wt% gold nanoparticles and rhodamine 6G; (ii) sporopollenin loaded with methylcellulose and rhodamine 6G; (iii) sporopollenin loaded with gold nanoparticles and rhodamine 6G; (iv) sporopollenin loaded with rhodamine 6G only. The concentration of rhodamine 6G was approximately 1×10^{-5} M in all samples. The samples were filtered, the residue was washed with 3.5 L of DI water and suspended into 0.5 mL of DI water in a UV cuvette. The samples were then exposed to the NIR laser light (806 nm, 1.5 W, beam radius 0.4 cm, 20 min exposure).

After the NIR laser irradiation, samples were filtered, and the absorbance of the rhodamine 6G was measured using UV-vis spectrophotometer.

2.2.7 Confocal laser scanning microscopy. Confocal laser scanning microscopy (CLSM) was carried out using (Carl Zeiss LSM780, Germany) providing laser lines (405/458/488/514/561/633 nm). Samples were mounted on a glass slide with a dimple in the middle, then a drop of pure water or alkaline medium (pH 8) was added before covering with a cover slip. Fluorescence from the samples was collected using laser excitation lines at 405 nm (2%) and 514 nm (2%) with DIC in Plan-Apochromat 20×/0.8 M27 objective lens. Fluorescence was collected with 410–492 nm and 528–678 nm emission filters and the optimal settings for the iris was used. Images were captured and processed using ZEISS ZEN 3.9 software (ZEISS, Germany).

3 Results and discussions

3.1 pH triggered release of rhodamine 6G

The encapsulation of the rhodamine-stained nanogel into the sporopollenin was done at low pH (4) where the nanogel is in its collapsed state. A tablet of compressed sporopollenin is was mixed with the carbopol nanogel formulation diluted with

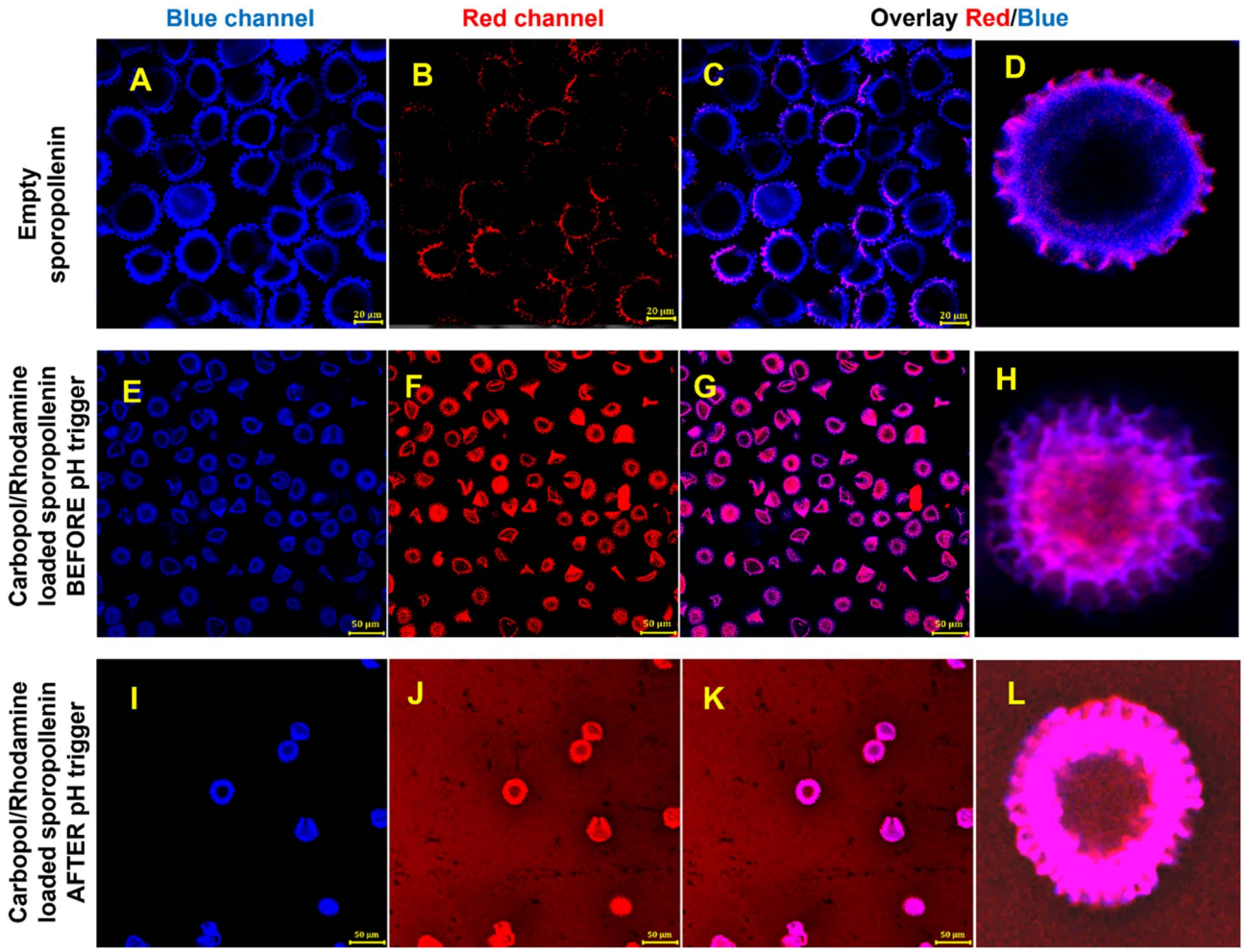

Fig. 2 (A)–(D) Confocal laser scanning microscopy (CLSM) images of an aqueous suspension of *Lycopodium clavatum* sporopollenin. The images show the autofluorescence of the sporopollenin with 405 nm (A), with 514 nm (B) and the overlay of these two channels in (C) and (D). (E)–(H) CLSM images of an aqueous suspension of *Lycopodium clavatum* sporopollenin loaded with Carbopol Aqua SF-1 nanogel stained with rhodamine 6G. The images are taken before pH trigger where the solution has a pH 4. The image (E) shows again a similar autofluorescence when excited at 405 nm but gives enhanced fluorescence upon excitation at 514 nm due to the rhodamine 6G payload. (I)–(L) CLSM images of an aqueous suspension of *Lycopodium clavatum* sporopollenin loaded with Carbopol Aqua SF-1 nanogel stained with rhodamine 6G after the pH trigger.

20 vol% absolute ethanol with magnetic stirring until complete dispersion of the tablet into the nanogel suspension. This causes the trilite scars of the elastic sporopollenin capsules which are largely open in the compressed tablet to recover their spherical shape and close, thus trapping the nanogel inside. Further degassing of the solution facilitates more complete loading. The role of the ethanol addition is to improve the wetting of the sporopollenin interior by the nanogel solution. Fig. S5 (ESI†) illustrates the steps of this process.[27]

The swelling behavior of Carbopol Aqua SF-1 nanogel against pH revealed that the average size of the polymer domains sharply rises above pH 6 reaching a maximum size of 320 nm at pH 7 and then slightly declines with further increases in the pH (Fig. S1, ESI†). The average size estimated from TEM of nanogel below pH 6 was around 100 nm as shown in (Fig. S1 and S2, ESI†). Based on these results, we expected the release of rhodamine 6G as a model drug can be triggered above pH 6 where the polymer expands, allowing the entrapped active to diffuse out of polymer chains. In addition, the released rhodamine 6G must diffuse either initially through the trilite scare (see Fig. S3C, ESI†), which might be a fast process, or through the nano channels on the wall of sporopollenin in a slow-release trend.

It is worth mentioning that these sporopollenin microcapsules have unique elastic and robust behavior where they recovered their original ornamental structure even after being compressed in a tablet at 10 tones. More brightfield and SEM images of sporopollenin derived from *Lycopodium clavation* can be seen in Fig. S3, ESI.†

Fig. 2 shows CLSM images of an aqueous suspension of sporopollenin before and after loading with Carbopol Aqua SF-1 nanogel stained with rodamine 6G (the first two rows of images). The third row of images shows the result of the pH trigger which leads to swelling and ejection of rhodamine 6G stained carbopol nanogel out of the sporopollenin. Note that increased background fluorescence when excited at 514 nm and its overlay images (Fig. 2J–L).

Fig. 3A shows a fluorescence microscopy image of the sporopollenin encapsulated with rhodamine 6G loaded nanogels suspended in pure water. The background appears black and the capsules red, which suggests that the dye is essentially concentrated in the capsules and that suspending the capsules into water did not induce the release. A drop of 0.1 M NaOH was then added and diffused through the water until it reached the spot exposed to the lens's focus. Once NaOH reached the exposed spot, a "flow" of red fluorescence could be immediately seen while recording images. This observation indicates that the nanogels swelled and the sporopollenin released the dye, as revealed by the increase in the fluorescence intensity in the background around the capsules, depicted in Fig. 3B. After the red fluorescence outflow passed, the background fluorescence intensity remained higher, which suggests that the release happened as shown in Fig. 3C for the suspension after the release. A typical movie was recorded showing the pH triggered release process (Videos S1 and S2, ESI†). The control experiment where the sporopollenin was loaded only with rhodamine 6G without the nanogels revealed that the fluorescence intensity

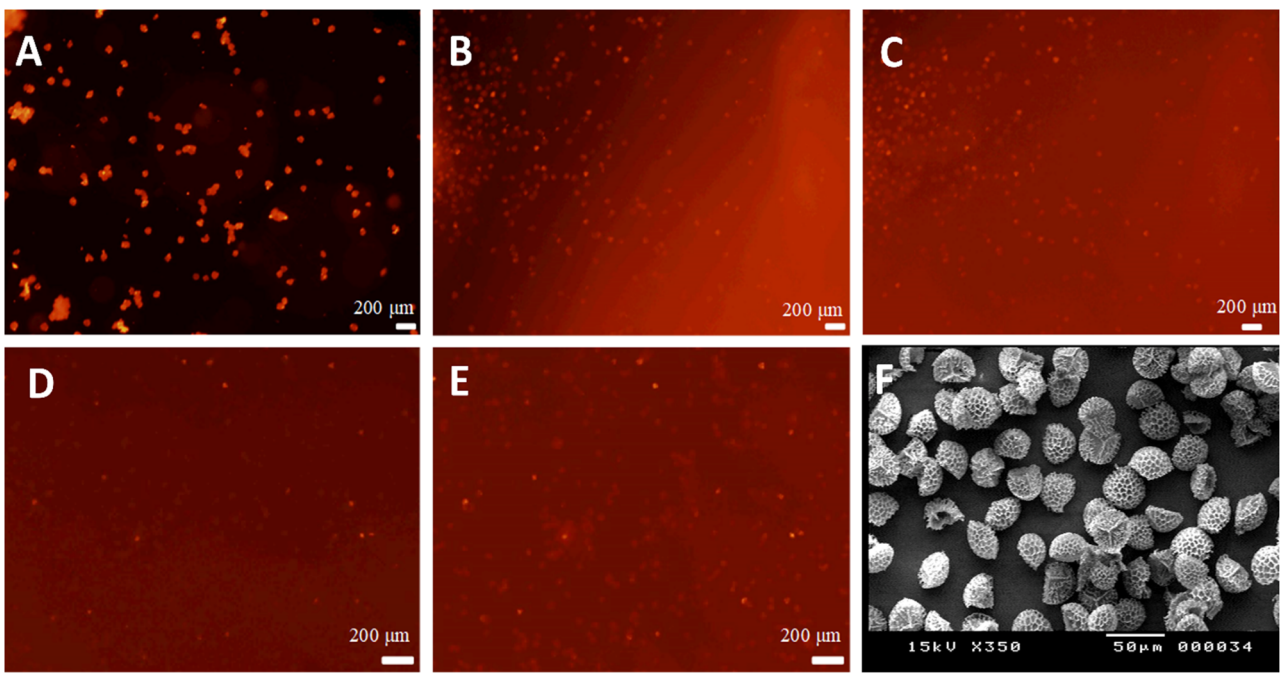

Fig. 3 (A) Fluorescence microscopy image of an aqueous suspension of *Lycopodium clavatum* sporopollenin loaded with a Carbopol Aqua AF-1 nanogel and rhodamine 6G followed by filtration. (B and C) The same system after addition of a drop of 0.1 M NaOH into a perfusion chamber. The front of higher pH is visualized in (B) with light intensity of fluorescence of the released rhodamine 6B. (D) Control experiment: Fluorescence microscopy image of an aqueous suspension of *Lycopodium clavatum* sporopollenin, after being loaded with rhodamine 6G solution (no carbopol nanogel) followed by filtration to remove excess dye. (E) The same system as (D) after addition of a drop 0.1 M NaOH into the perfusion chamber. The exposure time for all images (A)–(E) was 50.4 ms. (F) SEM image of the sporopollenin sample with clearly seen trilite scars.

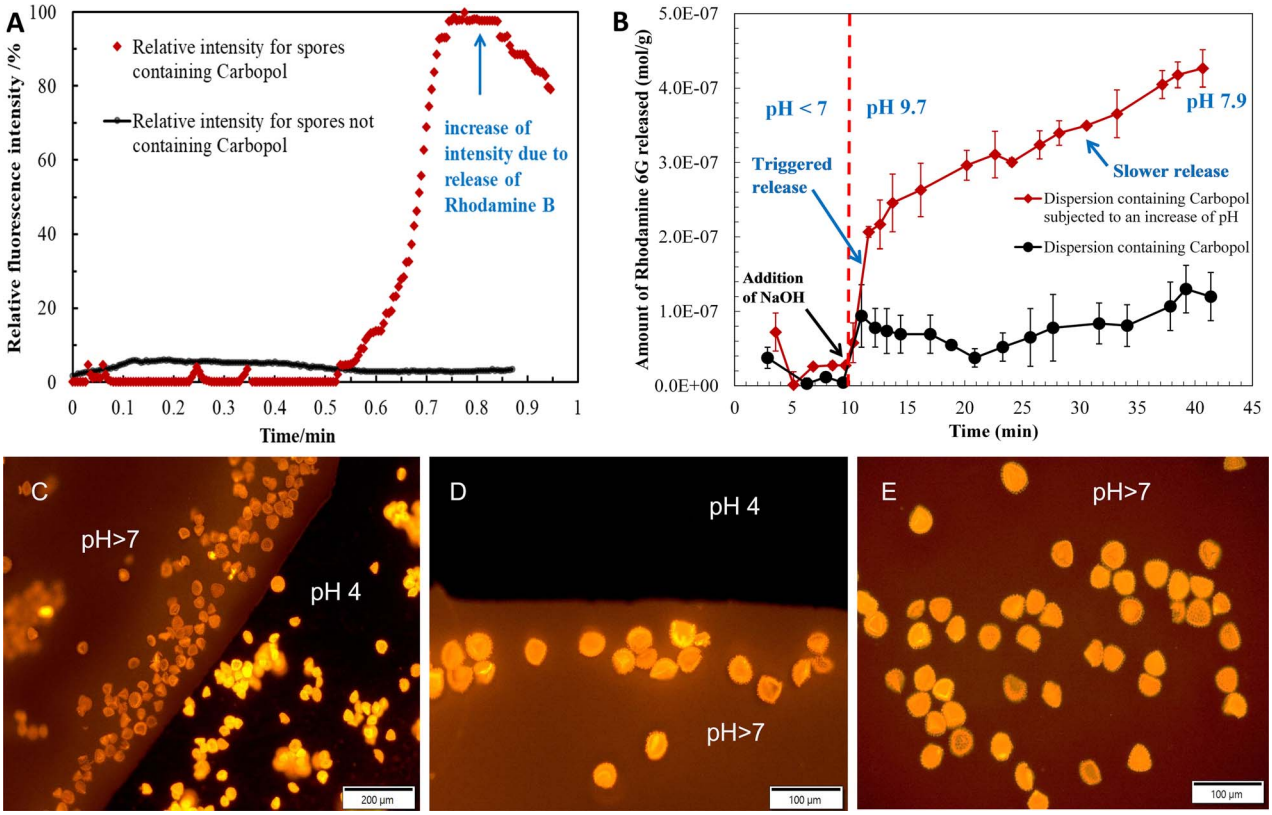

Fig. 4 (A) Relative average fluorescence intensity estimated from the microscopy image of a *Lycopodium clavatum* sporopollenin suspension (4 × 0.13) loaded with a Carbopol Aqua AF-1 nanogel and rhodamine 6G followed by filtration. (B) Amount of rhodamine 6G released as a function of time upon pH trigger. The system is equivalent to (A). Note the triggered release of the rhodamine 6G (by addition of 0.1 M NaOH) is followed by a slower rate as pH equilibrates in the solution. (C)–(E) Still fluorescence microscope images with TRITC filter set from videos like S1 and S2 (ESI†) of the process of adding of a drop of 0.1 M NaOH to a perfusion chamber with a suspension of sporopollenin loaded with Carbopol Aqua SF-1 stained with rhodamine 6B. The front of solution of pH > 7 causes the release of the carbopol due to swelling inside of the sporopollenin capsules leading to its ejection.

remains approximately constant before and after the addition of NaOH as shown in Fig. 3D and E, respectively.

It transpired that the presence of the carbopol nanogel provided a triggered release of the dye in a more controlled way. Fig. 3F shows sporopollenin microcapsules loaded with rhodamine 6G and nanogels using bright field optical microscopy. To further evaluate the pH triggered release profile of the dye, the fluorescent intensity and the released content of the dye were investigated. Fig. 4A illustrates the change of relative fluorescence intensity of the rhodamine 6G from sporopollenin suspensions with and without carbopol after the addition of one drop of 0.1 M NaOH. The average background fluorescence intensity of the first recorded images is the reference. It is evident that the presence of Carbopol Aqua SF-1 nanogel significantly contributed for the increased intensity and the triggered release where the relative intensity of the sample containing the nanogel passed through a maximum between 0.5 and 0.9 minutes. However, the relative intensity of the sample without the nanogel was significantly low (<10%) when compared to that with the nanogel within the same time intervals. Fig. 4B shows a typical graph of the amount of rhodamine 6G released with time. Additional runs of sporopollenin samples under identical conditions are presented in Fig. S4 (ESI†). The values in blue account for the pH of the dispersion subjected to an increase of pH. This deceleration of release may be due to uniform distribution of the NaOH over the volume of the chamber. The whole amount of dye does not seem to be released instantaneously after the addition of 0.1 M NaOH. The release is accompanied by an initial burst as soon as the NaOH solution front reaches them, as evidenced in Fig. 4C–E. However, the result may depend on the number of capsules in the chamber and the pH of the medium. The slow release could also be explained by diffusion of rhodamine 6G from the swollen carbopol nanogel inside the sporopollenin capsules to the surrounding liquid media. The total amount released after 40 minutes (in mol per gram of sporopollenin) is also slightly variable, approximately 4×10^{-7} mol g^{-1} for the first experiment, 8×10^{-7} mol g^{-1} for the second and 6×10^{-7} mol g^{-1} for the third one. These variations are due to the differences in the amount of sporopollenin placed in every beaker. In addition, the pH played a role in the slight variations.

3.2 Thermally triggered release

Methylcellulose exhibits unique thermal gelation behavior through chain–chain hydrophobic interactions and has a low

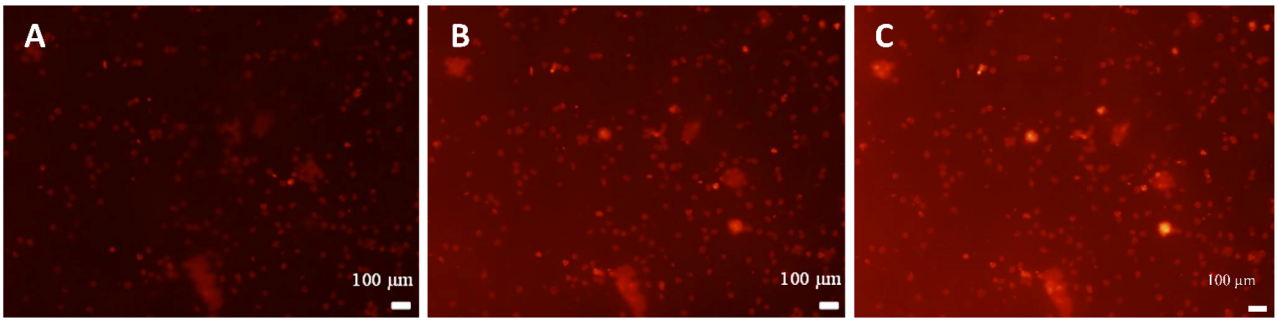

Fig. 5 (A) Fluorescence microscopy image of a *Lycopodium clavatum* sporopollenin suspension loaded with a methyl cellulose solution and rhodamine 6G followed by filtration. (B and C) The same system after heating to 66 °C and 80 °C, respectively. The exposure time for all images was 50.4 ms.

critical solution temperature (LCST) and thus transforms from a solution to a hydrogel as the temperature increased.[42] For optimization of loading the thermo-responsive polymer into sporopollenin, the effect of concentration and temperature on the average aggregate size and consistency of the methylcellulose particles was initially tested. The results obtained are summarized in (Table S1, ESI†). A gel-like consistency was seen for the 2 wt% methylcellulose while for a 1 wt% methylcellulose, slightly viscous suspension was obtained at 25 °C and 41 °C. It was reported that the lower critical solution temperature (LCST) of methylcellulose is about 30 °C where the solution exhibits Newtonian behavior below this temperature and becomes non-Newtonian above this point as shear rate increases.[41] A slightly viscous polymer solution was selected to allow a facile loading into the sporopollenin. The fluorescence microscope images in Fig. 5A–C illustrate the change of the fluorescence intensity with the temperature of the sporopollenin suspensions loaded with a methylcellulose solution and rhodamine 6G. One can see from Fig. 5A–C that the release of rhodamine 6G from the methylcellulose-loaded sporopollenin was triggered upon heating the suspension to 66 °C and 80 °C. A movie was recorded for this thermal responsive release at ~66 °C as shown in (Video S3, ESI†). For the control sample, where no methylcellulose was loaded, a slight increase was seen in the fluorescent intensity of the dye upon heating to ~66 °C (Video S4, ESI†).

Fig. 6A shows the relative background fluorescence intensity *versus* time for the sporopollenin suspensions with and without methylcellulose. It was found that in both suspensions, the intensity of fluorescence increases above 66 °C, while a significant increase in intensity (90%) was obtained for the methylcellulose loaded sample whereas it was (40%) for the unloaded sample. The results suggested that temperature thus seemed to induce the release of the dye even without methylcellulose which might be because of the effect of increased diffusion. Nevertheless, a larger amount of dye seems to be released for the sample containing methylcellulose (80%) when compared to that without methylcellulose (20%) as shown in Fig. 6B, indicative of the key role of the polymer in the active release process. Depending on MW and content, at high temperature (~70 °C) methylcellulose solution becomes turbid gel in a metastable state and can collapses with the exclusion of the solvent.[41] Furthermore, the content of rhodamine 6G released from sporopollenin loaded with methylcellulose as a function of the temperature was measured as shown in Fig. 7. A maximum amount of dye was released at around 55 °C. It was suggested that around this temperature, methylcellulose starts to form

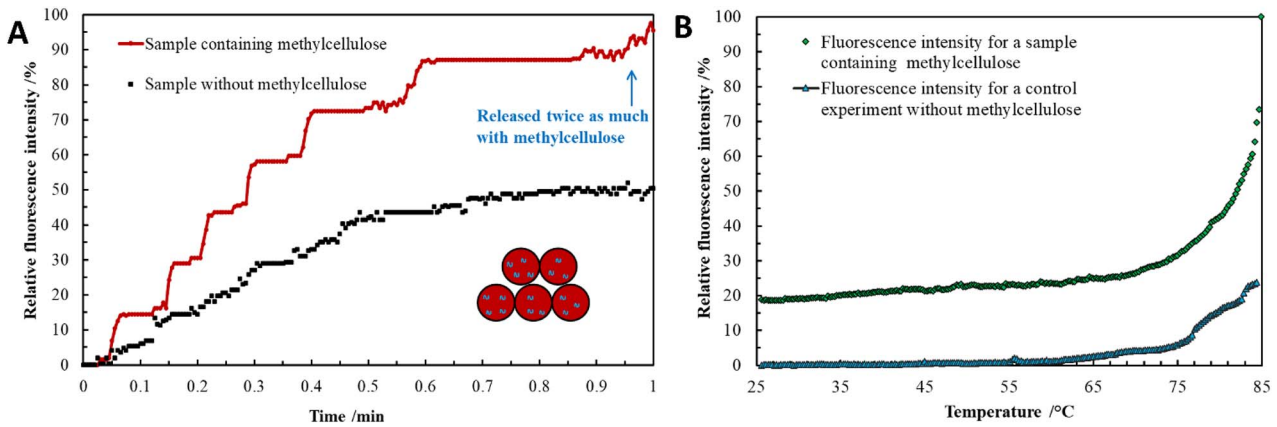

Fig. 6 (A) Relative fluorescence intensity due to release of rhodamine 6G with time after the increase of the temperature to 66 °C, with and without methylcellulose loaded in the sporopollenin microcapsules. (B) Relative fluorescence intensity due to release of rhodamine 6G as a function of the temperature.

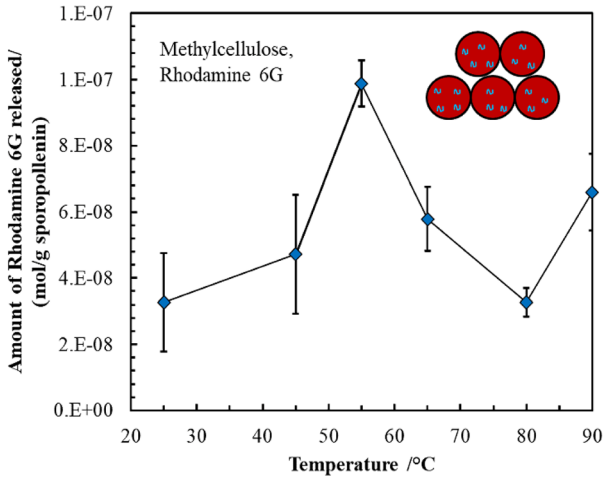

Fig. 7 Amount of rhodamine 6G released from sporopollenin loaded with methylcellulose and rhodamine 6G solution as a function of the temperature measured after incubation in a thermostat at the fixed temperature for 20 min.

aggregates with phase separation, independently of the molecular weight.[41]

The region below and above at the critical temperature (~30 °C), is thought to be the pre-gel stage. The underlying mechanism of gelation and phase separation of methylcellulose >50 °C, which is dependent on polymer structure, MW, degree of substitution and concentration is still not fully understood. Therefore, more viscoelastic sol–gel transition investigations are required to correlate the release trend with polymer gelation parameters.

3.3 NIR triggered active release

We also explored the photothermal properties of methylcellulose/rhodamine 6G solution doped with gold nanoparticles sporopollenin microcapsules *via* NIR irradiation. Light triggered release platforms have been used mainly *via* embedding gold or silver nanoparticles, NIR-dyes or carbon nanotubes within the shell of synthetic microspheres to eventually release the active through shell rupturing mechanism.[15–18] Here a different strategy was adopted using the unique properties of the natural and robust sporopollenin microcapsules. Fig. 8 shows that the amount of dye released form sporopollenin containing gold nanoparticles and methylcellulose is four times higher when compared to that with methylcellulose only, indicative of the key role of gold nanoparticles in providing local heat to trigger the release. Note that the gold nanoparticles are aggregated in the presence of methylcellulose solution. In addition, sporopollenin loaded with rhodamine 6G with or without gold nanoparticles showed comparable dye content released after irradiation but still not as high as the sample containing methylcellulose and gold nanoparticles. This further confirms the proof of principle of NIR-triggered release of the rhodamine 6G from the sporopollenin microcapsules loaded with thermo-sensitive polymer solution.

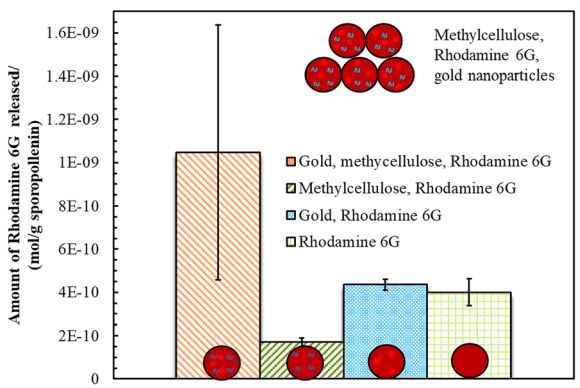

Fig. 8 Amount of rhodamine 6G released from sporopollenin loaded with (gold nanoparticles, methylcellulose and rhodamine 6G); (methylcellulose and rhodamine 6G); (gold nanoparticles and rhodamine 6G); (only rhodamine 6G). The readings are taken after irradiation with NIR laser (power 1.5 W, wavelength 806 nm, beam diameter 4 mm) for 20 min.

4 Conclusions

We demonstrated the feasibility of loading natural microcapsules derived from *Lycopodium clavatum* with different responsive biodegradable polymers, carbopol nanogel and methylcellulose for the development of smart microcapsules with the ability to fine-tune and control the release of actives in a non-destructive fashion. We describe the use of three different types of stimuli triggered release of rhodamine 6G as a model active from sporopollenin microcapsules based on pH sensitive, thermo-sensitive and near infrared light sensitive polymer composition. Carbopol nanogels prove that they can play a key role in the pH triggered release of a co-loaded active as revealed from fluorescent intensity and dye content results at different conditions. It is suggested that once the nanogels swell at pH > 6, the rhodamine 6G ejects together with them through the elastic trilite scare as well as through the nanochannels on the sporopollenin shell. Similar results were observed with thermally triggered release of active, co-encapsulated together with methyl cellulose upon heating to 55 °C. Photothermally triggered release using near infrared laser revealed that, for methylcellulose/gold nanoparticles composition, the active released from sporopollenin was four times higher than without gold nanoparticles, confirming their crucial role for photothermal trigger. We show that a non-destructive multiple-stimuli-responsive natural microcapsules can be developed where their properties can be easily tailored for a controlled and target release platform. The obtained smart natural microcapsules provided different stimuli-triggered action that can be customized for use in potential "on-demand" drug delivery and biomedical applications.

Author contributions

The manuscript was written through contributions of all authors. VNP gave the idea of the study, secured the funding, and supervised, directed the research and edited the manuscript. ML and JB performed the experiments, prepared the

figures and the first draft of the manuscript. AKFD provided technical guidance and images, co-drafted and edited parts of the manuscript. All authors have given approval to the final version of the manuscript.

Conflicts of interest

No conflicts of interest to declare.

Acknowledgements

ML acknowledges Ecole Nationale Supérieure de Chimie de Rennes for the opportunity to complete this work and the support from ERASMUS+ mobility grant. AKFD thanks Nazarbayev University for supporting his visiting professorship. VNP acknowledges his Nazarbayev University Faculty Development Competitive Research Grant (No. 11022021FD2909, VNP).

References

1 N. Choudhury, M. Meghwal and K. Das, Microencapsulation: An overview on concepts, methods, properties and applications in foods, *Food Front.*, 2021, **2**, 426–442.
2 C. Yan, S. R. Kim, D. R. Ruiz and J. R. Farmer, Microencapsulation for Food Applications: A Review, *ACS Appl. Bio Mater.*, 2022, **5**, 5497–5512.
3 F. Paulo and L. Santos, Design of experiments for microencapsulation applications: A review, *Mater. Sci. Eng., C*, 2017, **77**, 1327–1340.
4 A. Rana, M. Adhikary, P. K. Singh, B. C. Das and S. Bhatnagar, "Smart" drug delivery: A window to future of translational medicine, *Front. Chem.*, 2023, **10**, 1095598.
5 D. Liu, F. Yang, F. Xiong and N. Gu, The Smart Drug Delivery System and Its Clinical Potential, *Theranostics*, 2016, **6**, 1306–1323.
6 Y. Long, C. Liu, B. Zhao, K. Song, G. Yang and C. H. Tung, Bio-inspired controlled release through compression-relaxation cycles of microcapsules, *NPG Asia Mater.*, 2015, **7**, e148.
7 S. Mura, J. Nicolas and P. Couvreur, Stimuli-responsive nanocarriers for drug delivery, *Nat. Mater.*, 2013, **12**, 991–1003.
8 E. G. Kelley, J. N. L. Albert, M. O. Sullivan and T. H. Epps, Stimuli-responsive copolymer solution and surface assemblies for biomedical applications, *Chem. Soc. Rev.*, 2013, **42**, 7057–7071.
9 J. Wei, X. J. Ju, X. Y. Zou, R. Xie, W. Wang, Y. M. Liu and L. Y. Chu, Multi-stimuli-responsive microcapsules for adjustable controlled-release, *Adv. Funct. Mater.*, 2014, **24**, 3312–3323.
10 S. Zhang, Y. Zhou, W. Nie, L. Song, J. Li and B. Yang, Fabrication of uniform 'smart' magnetic microcapsules and their controlled release of sodium salicylate, *J. Mater. Chem. B*, 2013, **1**, 4331–4337.
11 Z. Chen, W. Zhou, Y. Wei, L. Shi, Z. Zhang, M. Dadgar, G. Zhu and G. Zhang, Preparation and performance of stimulus-responsive drug delivery system: a novel light-triggered temperature-sensitive drug-loaded microcapsules, *J. Mater. Chem. B*, 2023, **11**, 9757–9764.
12 A. L. White, C. Langton, M. L. Wille, J. Hitchcock, O. J. Cayre, S. Biggs, I. Blakey, A. K. Whittaker, S. Rose and S. Puttick, Ultrasound-triggered release from metal shell microcapsules, *J. Colloid Interface Sci.*, 2019, **554**, 444–452.
13 Z. Xiao, P. Sun, H. Liu, Q. Zhao, Y. Niu and D. Zhao, Stimulus responsive microcapsules and their aromatic applications, *J. Controlled Release*, 2022, **351**, 198–214.
14 Y. Niu, J. Wu, Y. Kang, Q. Zhao, Z. Xiao and D. Zhao, *Prog. Org. Coat.*, 2023, **176**, 107390.
15 A. M. Yashchenok, D. N. Bratashov, D. A. Gorin, M. V. Lomova, A. M. Pavlov, A. V. Sapelkin, B. S. Shim, G. B. Khomutov, N. A. Kotov, G. B. Sukhorukov, H. Möhwald and A. G. Skirtach, Carbon nanotubes on polymeric microcapsules: Freestanding structures and point-wise laser openings, *Adv. Funct. Mater.*, 2010, **20**, 3136–3142.
16 A. G. Skirtach, A. M. Yashchenok and H. Möhwald, Encapsulation, release and applications of LbL polyelectrolyte multilayer capsules, *Chem. Commun.*, 2011, **47**, 12736–12746.
17 W. Xu, I. Choi, F. A. Plamper, C. V. Synatschke, A. H. E. Müller and V. V. Tsukruk, Nondestructive light-initiated tuning of layer-by-layer microcapsule permeability, *ACS Nano*, 2013, **7**, 598–613.
18 R. Kurapati and A. M. Raichur, Near-infrared light-responsive graphene oxide composite multilayer capsules: A novel route for remote controlled drug delivery, *Chem. Commun.*, 2013, **49**, 734–736.
19 G. Mackenzie, A. N. Boa, A. Diego-Taboada, S. L. Atkin and T. Sathyapalan, Sporopollenin, the least known yet toughest natural biopolymer, *Front. Mater.*, 2015, **2**, 66.
20 Y. A. Maruthi and S. Ramakrishna, Sporopollenin - Invincible biopolymer for sustainable biomedical applications, *Int. J. Biol. Macromol.*, 2022, **222**, 2957–2965.
21 V. Aylanc, A. F. Peixoto, N. Vale, C. Freire and M. Vilas-Boas, Sporopollenin-based bio-microcapsules as green carriers for controlled delivery of pharmaceutical drugs, *Appl. Mater. Today*, 2023, **33**, 101860.
22 V. N. Paunov, G. Mackenzie and S. D. Stoyanov, Sporopollenin micro-reactors for in-situ preparation, encapsulation and targeted delivery of active components, *J. Mater. Chem.*, 2007, **17**, 609.
23 N. M. Meligi, A. K. F. Dyab and V. N. Paunov, Sustained in vitro and in vivo delivery of metformin from plant pollen-derived composite microcapsules, *Pharmaceutics*, 2021, **13**, 1048.
24 S. Iravani and R. S. Varma, Plant Pollen Grains: A Move Towards Green Drug and Vaccine Delivery Systems, *Nano-Micro Lett.*, 2021, **13**, 128.
25 M. J. Uddin, S. Liyanage, N. Abidi and H. S. Gill, Physical and Biochemical Characterization of Chemically Treated Pollen Shells for Potential Use in Oral Delivery of Therapeutics, *J. Pharm. Sci.*, 2018, **107**, 3047–3059.
26 N. M. Meligi and A. K. F. Dyab, Natural sporopollenin microcapsules: biological evaluation and application in

regulating hepatic toxicity of diclofenac sodium in vivo, *Biomater. Sci.*, 2023, **11**, 6193–6209.

27 S. A. Hamad, A. F. K. Dyab, S. D. Stoyanov and V. N. Paunov, Encapsulation of living cells into sporopollenin microcapsules, *J. Mater. Chem.*, 2011, **21**, 18018–18023.

28 K. Stamatopoulos, V. Kafourou, H. K. Batchelor and S. J. Konteles, Sporopollenin Exine Microcapsules as Potential Intestinal Delivery System of Probiotics, *Small*, 2021, **17**, 2004573.

29 J. Liu, X. D. Yan, X. Q. Li, Y. H. Du, L. L. Zhu, T. T. Ye, Z. Y. Cao, Z. W. Dong, S. T. Li, X. Xu, W. Bai, D. Li, J. W. Zhang, S. J. Wang, S. H. Li, J. Sun and X. Z. Yin, Chrysanthemum sporopollenin: A novel vaccine delivery system for nasal mucosal immunity, *Front. Immunol.*, 2023, **14**, 1132129.

30 N. Sudareva, O. Suvorova, N. Saprykina, A. Vilesov, P. Bel'Tiukov, S. Petunov and A. Radilov, Two-level delivery systems for oral administration of peptides and proteins based on spore capsules of *Lycopodium clavatum*, *J. Mater. Chem. B*, 2017, **5**, 7711–7720.

31 E. O. Asare, A. Seidakhanova, D. Amangeldinova, E. Marsili and V. N. Paunov, Targeting S. epidermidis Biofilms by the Tetracycline-Loaded Nanogel Surface Functionalized with Savinase, DNase, and Cellulase, *ACS Appl. Nano Mater.*, 2023, **6**, 22792–22806.

32 A. Diego-Taboada, S. Beckett, S. Atkin and G. Mackenzie, Hollow Pollen Shells to Enhance Drug Delivery, *Pharmaceutics*, 2014, **6**, 80–96.

33 A.-S. Y. Mohammed, A. K. F. Dyab, F. Taha and A. I. A. Abd El-Mageed, Encapsulation of folic acid (vitamin B9) into sporopollenin microcapsules: Physico-chemical characterisation, in vitro controlled release and photoprotection study, *Mater. Sci. Eng., C*, 2021, **128**, 112271.

34 V. Korzhikov-Vlakh and T. Tennikova, in *Advances in Biochemical Engineering/Biotechnology*, Springer Science and Business Media Deutschland GmbH, 2021, vol. 178, pp. 99–146.

35 S. Ahmed, K. Alhareth and N. Mignet, Advancement in nanogel formulations provides controlled drug release, *Int. J. Pharm.*, 2020, **584**, 119435.

36 K. S. Soni, S. S. Desale and T. K. Bronich, Nanogels: An overview of properties, biomedical applications and obstacles to clinical translation, *J. Controlled Release*, 2016, **240**, 109–126.

37 P. J. Weldrick, S. San and V. N. Paunov, Advanced Alcalase-Coated Clindamycin-Loaded Carbopol Nanogels for Removal of Persistent Bacterial Biofilms, *ACS Appl. Nano Mater.*, 2021, **4**, 1187–1201.

38 M. J. Al-Awady, A. Fauchet, G. M. Greenway and V. N. Paunov, Enhanced antimicrobial effect of berberine in nanogel carriers with cationic surface functionality, *J. Mater. Chem. B*, 2017, **5**, 7885–7897.

39 L. Bonetti, L. De Nardo and S. Farè, *Tissue Eng., Part B*, 2021, **27**, 486–513.

40 Y. H. Yeo, K. Chathuranga, J. S. Lee, J. Koo and W. H. Park, *Carbohydr. Polym.*, 2022, **277**, 118834.

41 P. L. Nasatto, F. Pignon, J. L. M. Silveira, M. E. R. Duarte, M. D. Noseda and M. Rinaudo, Methylcellulose, a Cellulose Derivative with Original Physical Properties and Extended Applications, *Polymers*, 2015, **7**, 777–803.

42 M. A. Ward and T. K. Georgiou, Thermoresponsive Polymers for Biomedical Applications, *Polymers*, 2011, **3**, 1215–1242.

43 E. O. Asare, E. A. Mun, E. Marsili and V. N. Paunov, Nanotechnologies for control of pathogenic microbial biofilms, *J. Mater. Chem. B*, 2022, **10**, 5129–5153.

44 P. J. Weldrick, M. J. Hardman and V. N. Paunov, Smart active antibiotic nanocarriers with protease surface functionality can overcome biofilms of resistant bacteria, *Mater. Chem. Front.*, 2021, **5**, 961–972.

45 M. J. Al-Awady, P. J. Weldrick, M. J. Hardman, G. M. Greenway and V. N. Paunov, Amplified antimicrobial action of chlorhexidine encapsulated in PDAC-functionalized acrylate copolymer nanogel carriers, *Mater. Chem. Front.*, 2018, **2**, 2032–2044.

46 P. J. Weldrick, S. Iveson, M. J. Hardman and V. N. Paunov, Breathing new life into old antibiotics: Overcoming antibacterial resistance by antibiotic-loaded nanogel carriers with cationic surface functionality, *Nanoscale*, 2019, **11**, 10472–10485.

47 P. J. Weldrick, A. Wang, A. F. Halbus and V. N. Paunov, Emerging nanotechnologies for targeting antimicrobial resistance, *Nanoscale*, 2022, **14**, 4018–4041.